Instrument Science Report WFC3 2017-20

Trace and Wavelength Calibrations of the UVIS G280 +1/-1 Grism Orders

Nor Pirzkal, Bryan Hilbert, Barry Rothberg

June 21, 2017

Abstract

We present new calibrations of the UVIS G280 grism dispersions for the -1 and +1 orders. The new calibration is based on in-flight observations of the star WR14 which was observed at multiple positions on the UVIS detector. This allowed us to derive a first estimate of the field dependence of the UVIS G280 dispersion. While previous, TV3 ground test based calibration, were only able to calibrate spectra obtained at the center of the UVIS CHIP1, our new solutions allow for the extraction and wavelength calibration of spectra over the entire UVIS field-of-view. We estimate the accuracy of the wavelength calibration using the new V2.0 dispersion solutions to be $\pm 7\mathring{A}$*, or about half of a UVIS resolution element.*

1. Introduction

The UVIS G280 grism offers a unique slitless mode spanning the wide wavelength range of approximately $2000 < \lambda < 8000\mathring{A}$. Unlike the WFC3 G102 and G141 grism however, the G280 spectra are strongly curved, multiple orders overlap at longer wavelengths, and the -1 is not well suppressed and is only about half as bright as the +1 order. It is therefore desirable to extract both the +1 and -1 order spectra of a source. The dispersion of the G280 grism was first calibrated using ground test TV3 data, as described in Kuntchner et al. (2009). Until now, the G280 grism was only calibrated near the center of CHIP1 and no field dependence had been derived. We use G280 observations of a calibration star (WR14), that were taken at multiple locations on both detectors, to derive new (V2.0) field dependent solutions for both the trace and wavelength solutions of the G280 grism in both CHIP1 and CHIP2. The calibration process is very similar to the one we performed for the IR G102 and G141 grism and extensive details about the fitting procedures are available in Pirzkal et al. (2016).

2. Field Dependence

The UVIS G280 grism suffers from a large amount of field dependence. The wavelength dispersions are different when the same source is observed in different parts of CHIP1 and CHIP2. Furthermore, where the sources lands on the detector is different in the G280 grism relative to where it would land through any other imaging filter. When applying a single unique (non-field varying) dispersion solution of the trace or of the wavelength to observations of a source in different parts of the field-of-view, large systematic errors are produced. This is shown in Figure 1 where we over-plot spectra of WR14 extracted from different parts off CHIP1. Large offsets in wavelengths are apparent as emission lines do not line up well. This is expected as we used the TV3 calibration of the G280 to extract and calibrate these spectra, and the TV3 calibration does not account for any field dependence.

3. Data

We used observations of the star WR14, obtained as part of proposals 12356, 12705, and 13091. These contained 24 and 22 spectra of WR14 taken at different positions of the CHIP1 and CHIP2 detectors, respectively. Figure 2 shows the positions at which WR14 was observed.

3.1. Trace Fitting

The spectra of WR14 have enough of a continuum level to allow us to measure and fit the trace of the multiple orders of the G280 spectra (see Figure 3). The trace measurements were done by computing the centroid of the trace as a function of x-pixel on the detector. Trace for each of the 46 available spectra were thus measured and fitted using a high-order 2D polynomial (see Equation 1 in Pirzkal et. al 2016). The best fit to the shape of the

G280 curved spectra was achieved using a 6^{th} order trace polynomial with a linear 2D field dependence. Figure 4 shows an example of one trace of a +1 order spectra. Being able to fit the trace correctly at the blue end, where the spectrum curves up, and at the red end, where the spectrum is essentially linear, required fine tuning the center of the polynomial description. The latter is shown using a vertical black line in Figure 4. Selecting a point close to the inflection point of the spectrum works best. Comparing our 2D polynomial fits to the original 46 trace measurements, we find that the model reproduces the location of the curved traces of the +1 and -1 order spectra to within a fraction of a pixel. We are also able to fit the trace over a larger span, fitting a longer portion of the red part of each spectra. Overall, the new V2.0 trace description is a significant improvement over that of the previous TV3 calibration, even at the center of CHIP1 where the original TV3 calibration was performed. The improvement is, in part, due to the use of a higher order trace description polynomial (The TV3 trace description used a 4^{th} order trace polynomial). Using the TV3 calibration, the location of spectra are offset by as much as 3 pixels, which is significant for the G280 grism.

Table 5 summarizes the RMS between observations and our new V2.0 trace model as well as the previous TV3 trace model, and show the significant improvement obtained using the V2.0 calibration.

3.1.1. Fiducial Wavelengths and Fitting

The spectra from Willis et al. (1986) and Crowther et al. (2002) were used to identify and measure the center of strong emission lines at wavelengths ranging from $1900 < \lambda < 8000\mathring{A}$. The fiducial wavelengths of these lines are listed in Table 2. The wavelength of these fiducial lines were measured by Gaussian fitting of the reference spectra. Examples of +1 and -1 order spectra and identified emission lines are shown in Figure 5. The procedure to extract and fit emission lines closely follows what was described in Pirzkal et al. (2016). We found that a 4^{th} order wavelength polynomial, with a linear 2D field dependence optimally fitted the observations for both CHIP1 and CHIP2 detectors and for both the +1 and -1 orders.

We extracted the WR14 observations using aXe with our new trace and wavelength calibrations of the +1 and -1 orders of CHIP1 and CHIP2. The same data were extracted using the TV3 trace and wavelength calibration to serve as a reference (see Figure 1. Figure 6 presents a qualitative comparison of the wavelength accuracy of the new V2.0 calibration and the previous TV3 calibration. The improved trace calibration allowed us to wavelength calibrate the spectra up to a wavelength of $\approx 8000\mathring{A}$, while previous TV3 calibration was restricted to $\approx 6000\mathring{A}$. These plots demonstrate the significant improvement in the recovered line wavelengths using the V2.0 calibration. Figures 7 and 8 show the difference between the fiducial WR14 line wavelengths (from Table 2) and the line wavelengths we measured by Gaussian fitting emission lines in the extracted and calibrated spectra. The V2.0 G280 calibration have a maximum wavelength error that is within $14\mathring{A}$ over the entire field of view of CHIP1 and CHIP2 (Right Panels in Figures 7 and 8 and Table 3).

4. Sample Configuration

The UVIS G280 +1 and -1 order calibrations were generated in the aXe Configurations files format, similarly to those generated for the WFC3 IR G102 and G141 grisms. The trace equation is:

$$\begin{aligned}\Delta y(x_0, y_0, \Delta x) = \; & b_{0,0} + b_{0,1} \times x_0 + b_{0,2} \times y_0 \\ & + \Delta x \times (b_{1,0} + b_{1,1} \times x_0 + b_{1,2} \times y_0) \\ & + \Delta x^2 \times (b_{2,0} + b_{2,1} \times x_0 + b_{2,2} \times y_0) \\ & + \Delta x^3 \times (b_{3,0} + b_{3,1} \times x_0 + b_{3,2} \times y_0) \\ & + \Delta x^4 \times (b_{4,0} + b_{4,1} \times x_0 + b_{4,2} \times y_0) \\ & + \Delta x^5 \times (b_{5,0} + b_{5,1} \times x_0 + b_{5,2} \times y_0) \\ & + \Delta x^6 \times (b_{6,0} + b_{6,1} \times x_0 + b_{6,2} \times y_0)\end{aligned} \tag{1}$$

The polynomial parameters describing the trace and wavelength dispersion of the CHIP1 +1 order are shown below. The aXe format trace coefficients are defined such that DYDX_A_i lists the three values of $b_{i,0}, b_{i,1}, and b_{i,2}$. The first three coefficients $b_{0,0}, b_{0,1}, and b_{0,2} therefore have the values o$ respectively. Similarly, the wavelength equation is:

$$\begin{aligned}\lambda(x_0, y_0, \Delta p) = \; & \lambda_{0,0} + \lambda_{0,1} \times x_0 + \lambda_{0,2} \times y_0 \\ & + \Delta p \times (\lambda_{1,0} + \lambda_{1,1} \times x_0 + \lambda_{1,2} \times y_0) \\ & + \Delta p^2 \times (\lambda_{1,0} + \lambda_{1,1} \times x_0 + \lambda_{1,2} \times y_0) \\ & + \Delta p^3 \times (\lambda_{1,0} + \lambda_{1,1} \times x_0 + \lambda_{1,2} \times y_0) \\ & + \Delta p^4 \times (\lambda_{1,0} + \lambda_{1,1} \times x_0 + \lambda_{1,2} \times y_0)\end{aligned} \tag{2}$$

and the $\lambda_{i,0}$ are listed by DLDP_A_i below.

```
#
# +1st order (BEAM A) ************************************
#
BEAMA -400 215
```

```
MMAG_EXTRACT_A 35
MMAG_MARK_A 35

#
# Trace description
#
DYDX_ORDER_A 6
DYDX_A_0 173.93329566558168  -0.0017745578583666709  0.004094178735199138
DYDX_A_1 -0.0037958978799161906  -1.4395595073604493e-6  -4.9509874353862106e-6
DYDX_A_2 0.0003335741958191544  -1.1591924817665047e-8  -1.2729699153070891e-10
DYDX_A_3 2.40209868635139e-6  -6.865066680530258e-11  -3.400404437206059e-11
DYDX_A_4 1.0550532737983465e-8  -2.0223735221418172e-13  -2.5330874248205076e-13
DYDX_A_5 2.199208773850666e-11  -1.9048302258762925e-16  -6.415473132470955e-16
DYDX_A_6 1.7135622752880473e-14  1.369061044996829e-19  -5.680791733691364e-19

#
# X and Y Offsets
#
XOFF_A -150
YOFF_A 0.0

#
# Dispersion solution
#
DISP_ORDER_A 4
DLDP_A_0 3547.8136743387913  0.04898603983516115  -0.027071680330018
DLDP_A_1 -13.75918635808393  -0.0002580304290965832  0.0001782486196050317
DLDP_A_2 0.005186011738915429  -4.058373100326685e-7  1.4895162535452872e-7
DLDP_A_3 0.000027969319182900263  1.1703833719297967e-10  -1.6241444481315035e-9
DLDP_A_4 4.6081199020831976e-8  3.9091305437750505e-12  -6.227527990849325e-12
SENSITIVITY_A wfc3_abscal_UVg280_1st_sensTV3.fits
```

The new calibration files are available at `http://www.stsci.edu/hst/wfc3/analysis/grism_obs/calibrations/wfc3_g280.html`.

5. Conclusion

We performed a full calibration of the trace and wavelength dispersion relations for the +1, and -1 orders of the G280 WFC3/UVIS grism on both the CHIP1 and CHIP2 detectors. The new dispersion solutions were derived using observations of the star WR14 obtained at multiple positions on the detectors. The V2.0 calibration allow for the extraction of UVIS +1 and -1 order spectra from any position on CHIP1 and CHIP2. The accuracy of the wavelength calibration is $\pm 7\mathring{A}$ over the entire field of view of both CHIP1 and and CHIP2.

REFERENCES

Crowther, P. A., Dessart, L., Hillier, D. J., Abbott, J. B., & Fullerton, A. W. 2002, A&A, 392, 653

Kuntschner H., Bushouse H., Kmmel M., Walsh J. R. *The ground calibrations of the WFC3/UVIS G280 grism*, WFC3-2009-01

Pirzkal, N., R. Ryan, and G. Brammer, *Trace and Wavelength Calibrations of the WFC3 G102 and G141 IR Grisms*, WFC3-2016-15

Willis, A. J., van der Hucht, K. A., Conti, P. S., & Garmany, D. 1986, A&AS, 63, 417

Table 1:: RMS of the trace residuals (pixel)

	CHIP1	CHIP2	CHIP1	CHIP2
Model	+1 Order		-1 Order	
V2.0	0.5	0.2	0.7	0.8
TV3 (Center)	0.5		2.0	
TV3	2.7	2.1	3.0	2.5

Trace residuals (in pixel) between observations and the V2.0 and previous TV3 calibration solutions. Near the center of CHIP1, the TV3 trace residuals are small for CHIP1 but significant for CHIP2. The large amount of field dependence of the G280 grism is visible when applying the TV3 calibration to the whole instrument with errors on the order of several pixels. The V2.0 trace calibration retains sub-pixel accuracy over the whole detector

Table 2:: Fiducial Emission Lines Wavelength for WR14

Emission Line Centers ($\AA$)					
1643.9	1911.0	2299.2	2402.6	2527.4	2906.0
3067.0	3704.8	3932.9	4073.7	4334.2	4444.0
4654.6	5131.1	5813.4	6569.7	6744.9	7059.7
7218.8	7729.0				

Fiducial emission line wavelengths used to calibrate the UVIS G280 observations. These lines were measured from the spectra of Willis et al. (1986) and Crowther et al. (2002). .

This preprint was prepared with the AAS LaTeX macros v4.0.

Table 3:: Errors in measured line wavelengths

	CHIP1	CHIP2	CHIP1	CHIP2
Model	+1 Order		-1 Order	
V2.0	5.1$\AA$	7.1$\AA$	5.1$\AA$	7.4$\AA$
TV3	29.0$\AA$	38.5$\AA$	30.6$\AA$	27.6$\AA$

Standard deviation of the difference between fiducial and observed emission line wavelengths when the WR14 data were extracted using the V2.0 and the TV3 trace and wavelength solutions over multiple positions on CHIP1 and CHIP2.

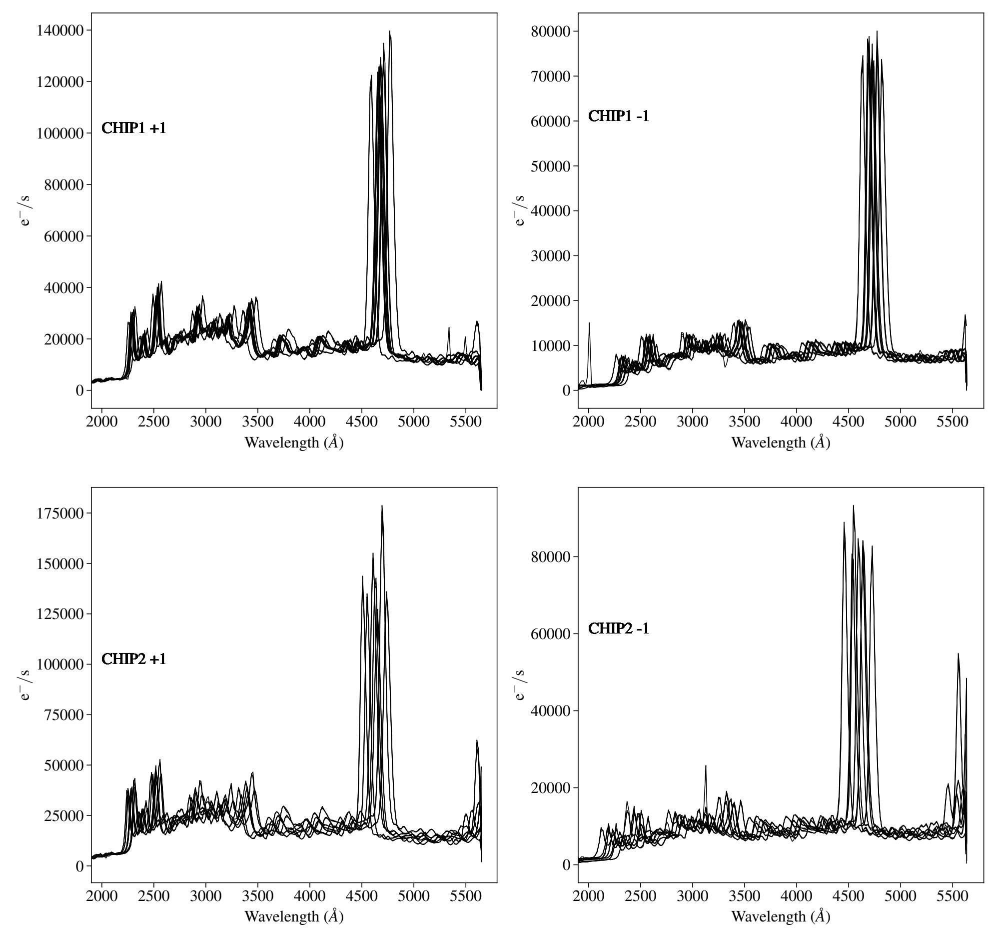

Fig. 1.—: UVIS G280 spectra of WR14. These were extracted using the previous dispersion calibration of the G280 grism (WFC3.UV.CHIP1.TV3_sim.conf). A total of 22 and 20 +1 and -1 order spectra in CHIP1 and CHIP2, are plotted, respectively. Since this calibration was determined only for the center position of CHIP1 and since the UVIS G280 has significant field dependence, the disagreement in wavelengths is expected. Clearly, using the TV3 center-of-chip trace and dispersion solution fails to produce spectra with consistent wavelength calibration. Significant wavelength offsets exist between spectra extracted on different part of CHIP1 and CHIP2.

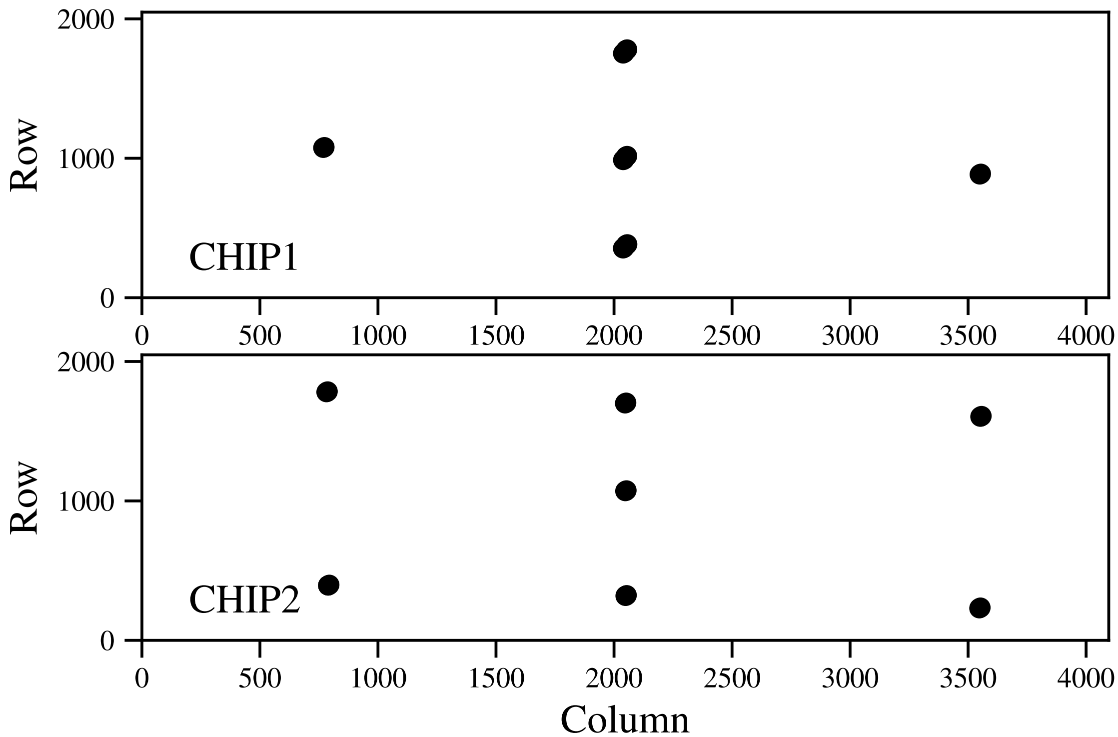

Fig. 2.—: Positions at which WR14 was observed in the UVIS CHIP1 and CHIP2 detectors. A total of 24 spectra were obtained in CHIP1 and 22 spectra in CHIP2.

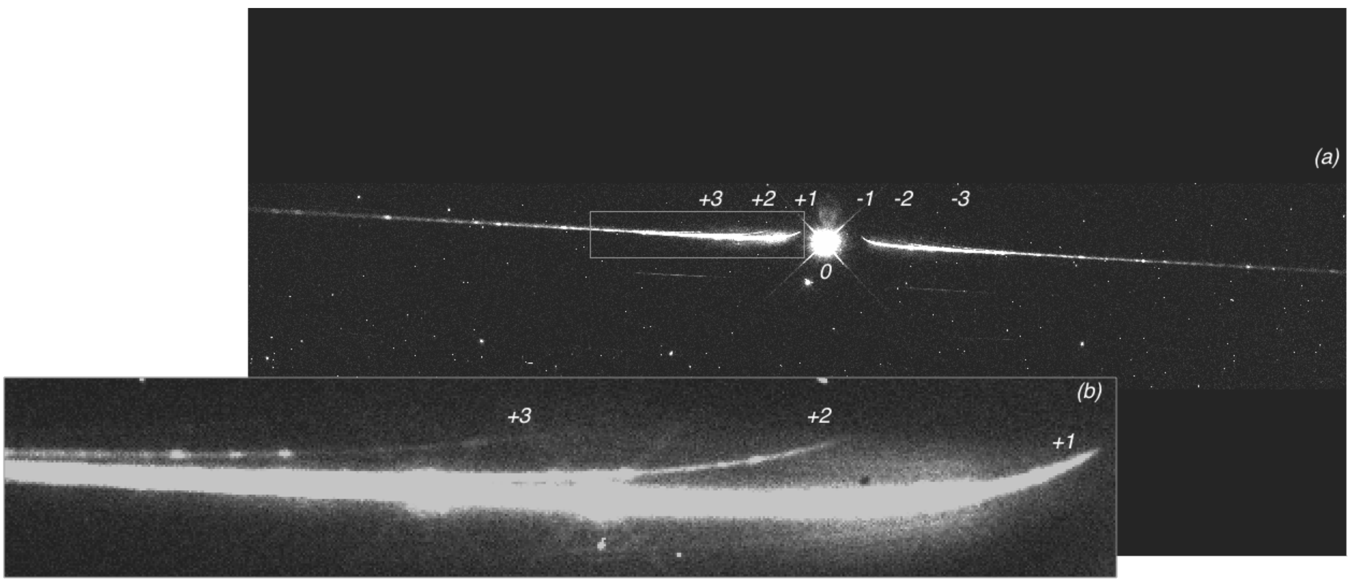

Fig. 3.—: UVIS G280 spectrum of WR14. Several orders are labeled. As shown here, the dispersed spectra are highly curved at lower wavelengths (right hand side of panel (b) and overlap at longer wavelengths where they merge.

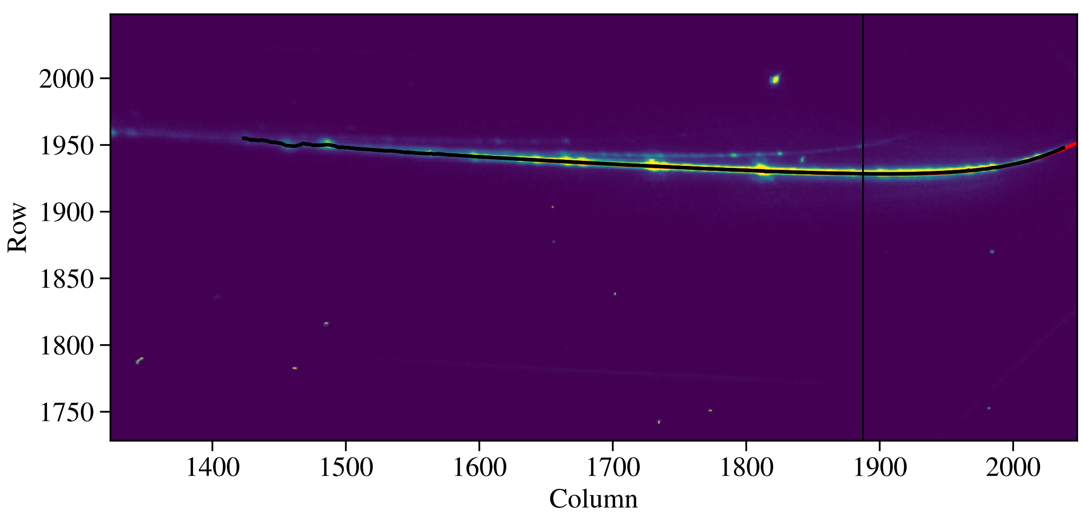

Fig. 4.—: Measurements of the position of the spectral trace of one of the +1 order of WR14 (black points). The final polynomial fit to the trace is also shown in red and very closely follows the trace measurements. The vertical black line is the chosen location of the polynomial reference column and is close to the inflection point of the trace.

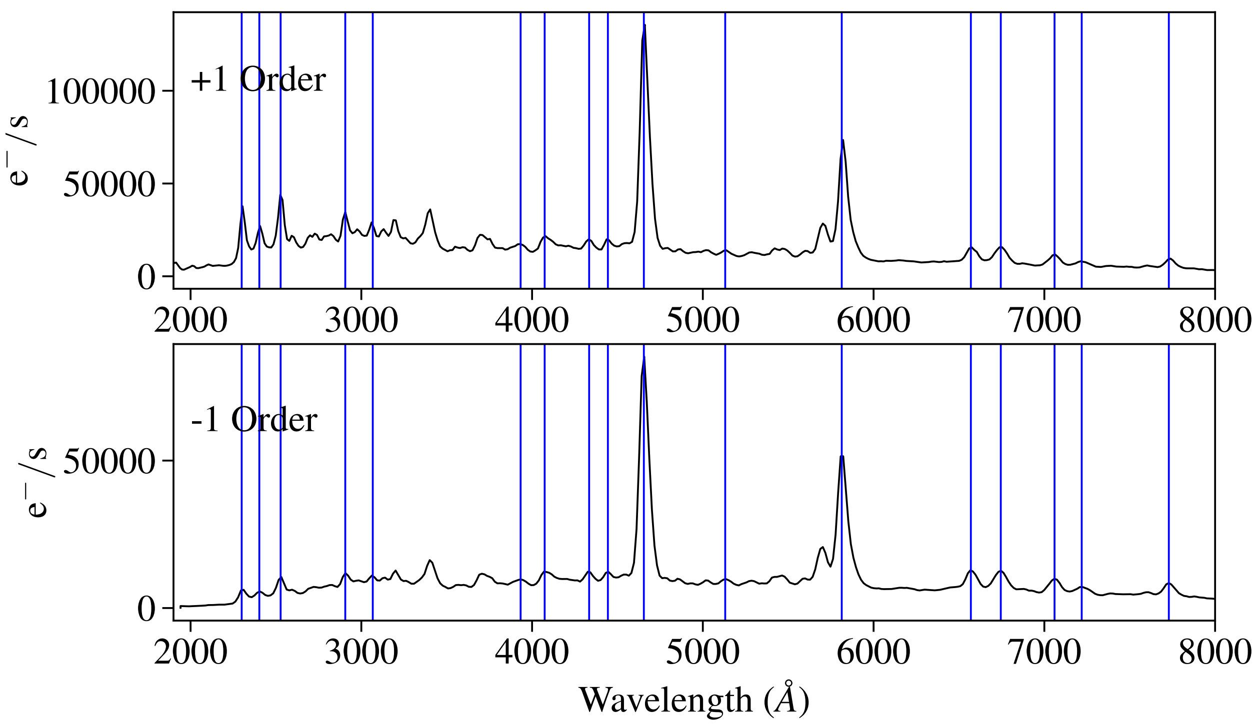

Fig. 5.—: +1 order (Top panel) and -1 order (Bottom panel) extracted spectra of WR14. The emission lines from Table 2 are shown. Bright emission lines can be detected from $2000 < \lambda < 8000\AA$.

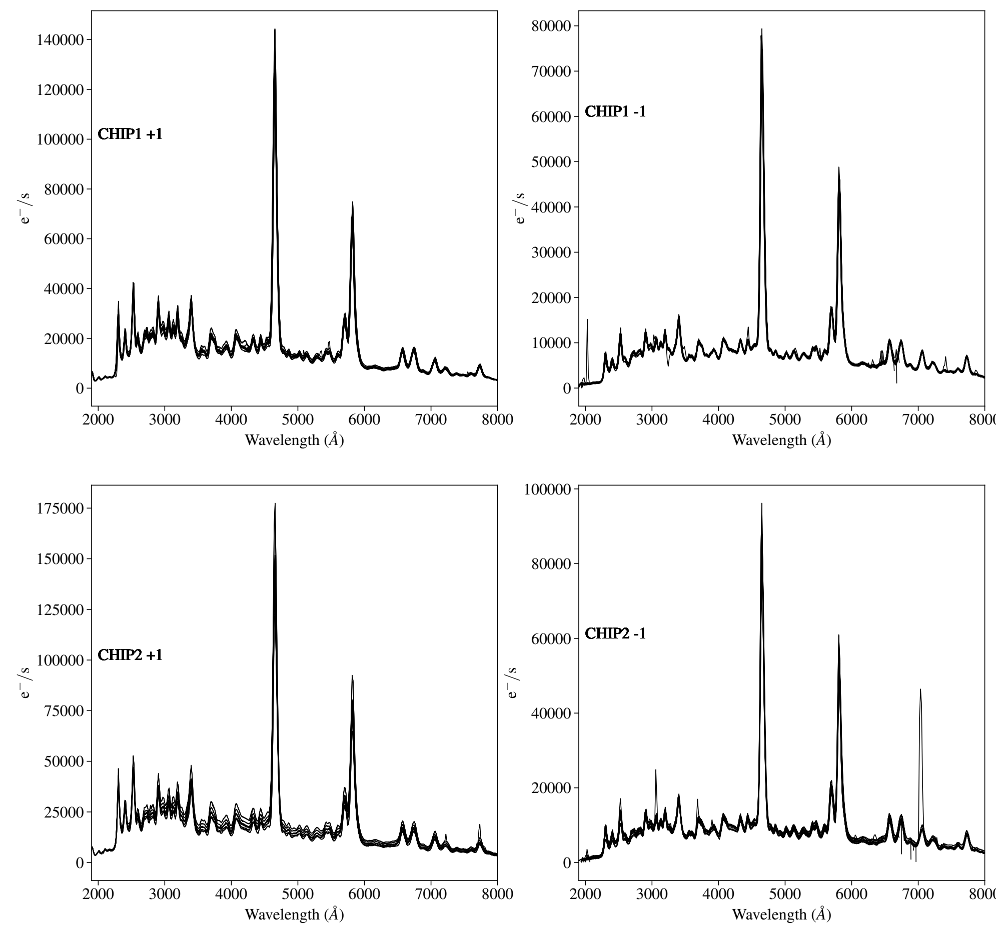

Fig. 6.—: Qualitative comparison of the trace and wavelength calibrations of UVIS G280 spectra of WR14. These were extracted using the V2.0 calibration of the trace and wavelength dispersion of the G280 grism (WFC3.UVIS.G280.CHIP1.V2.0.conf and WFC3.UVIS.G280.CHIP2.V2.0.conf). A total of 22 and 20 +1 and -1 order spectra in CHIP1 and CHIP2, are plotted, respectively. This figure can be directly compared to Figure 1 and shows a tigher agreement between all the extracted spectra as well as the increased wavelength span of the calibrated data. The disagreement in flux on the blue sides of the spectra is expected and caused by the highly curved nature of the spectra, resulting in self-contamination that is not corrected for.

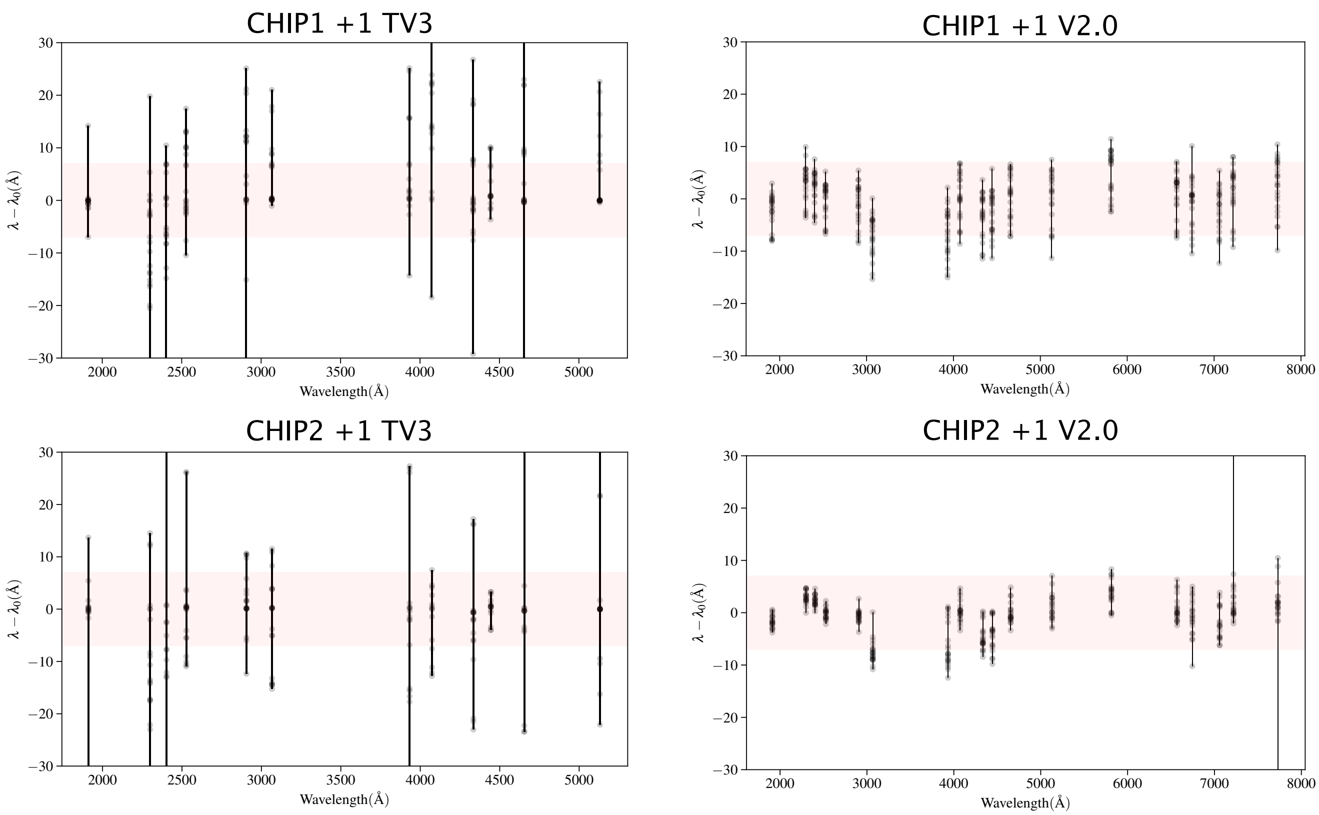

Fig. 7.—: (left) The error in emission line wavelengths when using the TV3 calibration to extract the +1 order spectra from CHIP1 and CHIP2 (top and bottom). (right) The error in emission line wavelengths when using V2.0 to extract the +1 order spectra (top and bottom) The shaded region represents one G280 resolution element (14Å).

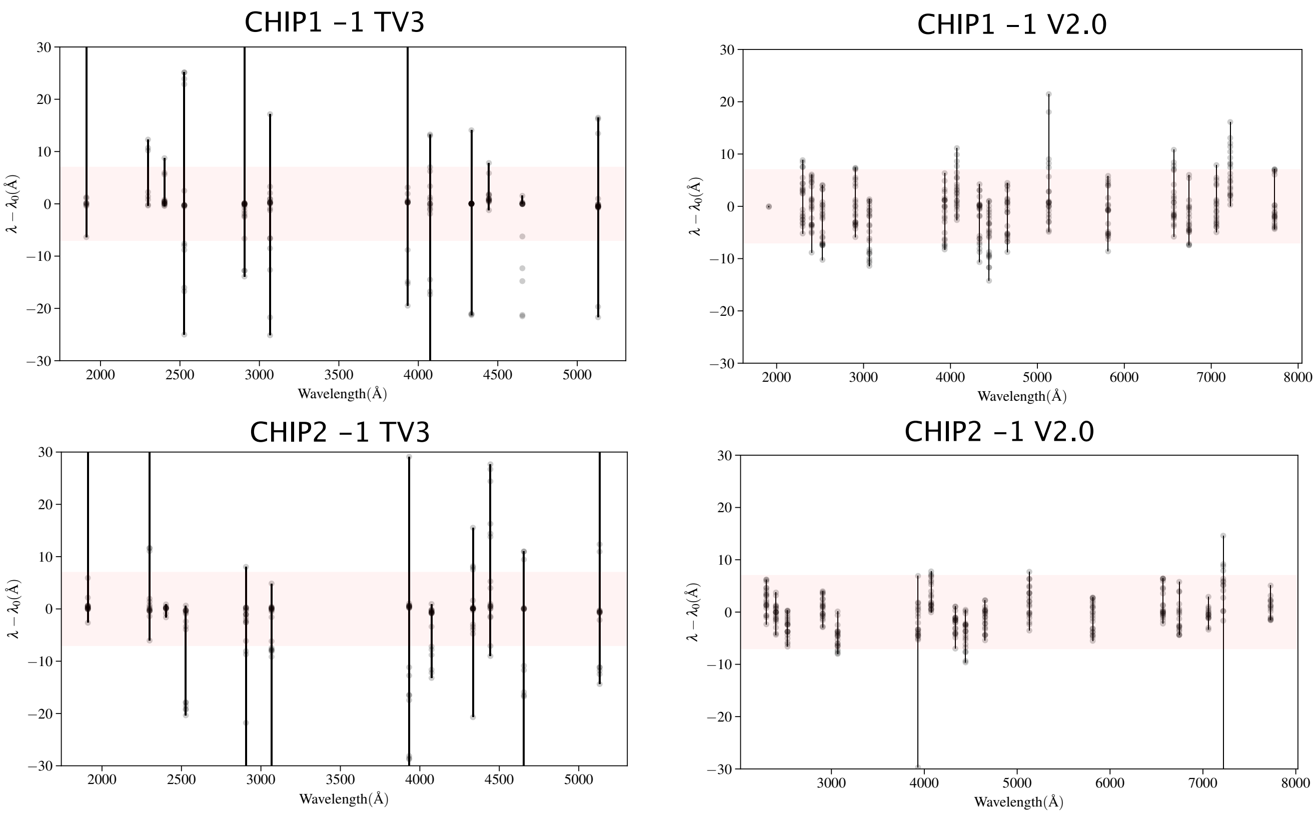

Fig. 8.—: (left) The error in emission line wavelengths when using the TV3 calibration to extract the -1 order spectra from CHIP1 and CHIP2 (top and bottom). (right) The error in emission line wavelengths when using V2.0 to extract the -1 order spectra (top and bottom) The shaded region represents one G280 resolution element (14$\AA$).